THE ROLES OF GEOMETRY AND TOPOLOGY STRUCTURES OF GRAPHITE FILLERS ON THERMAL CONDUCTIVITY OF GRAPHITE/ALUMINUM COMPOSITES

Cong Zhou [a], Dong Chen [a], Xiaobo Zhang [a], Zhe Chen [a*], Gang Ji [b*], Haowei Wang [a]

[a]*State Key Laboratory of Metal Matrix Composites, Shanghai Jiao Tong University, Shanghai 200240, China*
[b]*Unité Matériaux et Transformations, CNRS UMR 8207, Université Lille 1, Villeneuve d'Ascq 59655, France*
**e-mail addresses: zhe.chen@sjtu.edu.cn (Z. Chen); gang.ji@univ-lille1.fr (G. Ji)*

Keywords: Metal matrix composites; Graphite; Thermal conductivity; Analytical modeling

Abstract

Graphite fillers such as graphite particles, graphite fibers, graphite flakes, and porous graphite blocks have successfully been introduced to an Al-7wt.%Si alloy by squeeze casting to fabricate various graphite/Al composites with enhanced thermal conductivity (TC). Microstructure characterization revealed a tightly-adhered, clean and Al_4C_3-free interface between the graphite and the Al matrix. Taking into account the observed microstructural features, we generalized the corresponding predictive models for the TC of these composites with the effective medium approximation and the Maxwell mean-filed scheme. The predictions for the TC of the composites were in good agreement with the experimental data. The roles of geometry and topology structures of the fillers on the TC of the composites were further discussed.

1. Introduction

Metal matrix composites reinforced with graphite fillers, namely graphite/metal composites, are attractive materials, showing excellent thermal performance, and are currently used as heat sinks in electronic packaging systems [1]. For example, graphite/Al composites exhibit relatively high thermal conductivity (TC), low coefficient of theraml expansion (CTE) and good machinability [2]. To date, several graphite fillers (graphite particles, graphite fibers, graphite flakes, graphite foam, etc.) have been mixed with Al alloys through various fabrication techniques (squeeze casting, spark plasma sintering, vacuum hot pressing, etc.) to fabricate highly thermally conductive composites [2-5]. However, in reality the TCs of these composites are not as high as expected by theoretical predictions. Some believe that interfacial thermal resistance can be predominantly responsible for this, since undesirable excessive formation of aluminum carbide (Al_4C_3) can hinder effective heat transfer cross the graphite/Al interface due to low TC of Al_4C_3 itself [3,5,6]. Moreover, a molecular dynamics simulations study [7] recently showed that the aspect ratio and agglomeration of graphite fillers are more significant than the interfacial thermal resistance contributing to the global TC of the composites. This theoretical result highlighted that the

geometry and topology structures of graphite fillers can be the key factors to determine the TC of the composites. Especially, in the case of an Al_4C_3-free interface, the effect of the structure factors could be even more important and need to be systematically investigated. Unfortunately, to our knowledge, no enough attention has been paid to this issue so far.

The aim of this work is to study the influence of the geometry and topology structure factors of graphite fillers on the TC of the composites and evaluate their potentials. Graphite fillers with different forms (i.e. particle, fiber, flake and porous block) were incorporated in an Al-7wt.%Si alloy by squeeze casting processing. Besides, we generalized corresponding predictive models for the TC of the composites taking into account the observed microstructural features.

2. Experimental

The starting materials consisted of graphite fillers (i.e., graphite particles, graphite fibers, graphite flakes, and porous graphite block), an Al-7Si alloy and Si particles. Their thermo-physical properties are given in Table 1. Graphite flakes have a TC of about 1000 W/m K along the basal (i.e. xy) plane according to molecular dynamics simulations [3]. However, the TC perpendicular to the basal (i.e. z) plane is only 38 W/m K. Graphite fibers have the second highest TC of 700 W/m K along the fiber axis (i.e. z) direction. Comparatively, graphite particles and porous graphite block have isotropic and relatively low TCs. Fully-dense graphite/Al-7Si composites were produced by squeeze casting processing. Si particles were used as spacers in the graphite flakes case. More details of the fabrication process can be found in [8].

Starting materials	Density [g/cm^3]	TC [W/m K]
Graphite particles	2.26	100
Graphite fibers	2.15	xy: 12, z: 700
Graphite flakes	2.26	xy: 1000 [3], z: 38 [5]
Porous graphite block	1.74-1.85	154-168
Al-7Si alloy	2.68	151
Si particles	2.33	150

Table 1. Density and TCs of the starting materials used for the fabrication of the graphite/Al-7Si composites.

Microstructure characterization was carried out with scanning electron microscopy (SEM) and X-ray diffraction (XRD). A JEOL JSM-7600F instrument was used for SEM examinations. XRD measurements were performed on a D8 ADVANCE X-Ray diffractometer, operating at 40 kV/40 mA and using Cu K_α radiation (λ=0.15406 nm). TCs of the specimens (Ø 12.6 × 2 mm) were measured by a laser-flash method (LFA 447, NETZSCH).

3. Results and discussion

3.1 Microstructures

Fig. 1 illustrates the different morphologies of the graphite fillers. Graphite particles are irregular

in shape and appear aggregation to some extent (Fig. 1a). Graphite fibers have an average diameter of about 10 μm and an average length of about 400 μm (Fig. 1b). Graphite flakes, with an average diameter of about 500 μm and an average thickness of about 20 μm (Fig. 1c), display a neat platelet morphology. Porous graphite block has interconnected pores visible on its fracture surface (Fig. 1d). Fig. 2 shows the spatial distributions of the graphite fillers in the as-obtained graphite/Al-7Si composites. As shown in Figs. 2a and b, graphite particles are homogenously embedded in the Al-7Si alloy matrix, while graphite fibers present preferential directions (mostly perpendicular to the pressing direction). The orientation is caused by the applied pressing pressure during the fabrication process. The elongated dark regions in Fig. 2c represent the graphite flakes while the rest bright ones are the Si/Al-7Si material matrix. The layers of graphite flakes are stacked mostly parallel to each other and separated by the added Si particles. Fig. 2d illustrates the microstructure of the porous graphite block/Al-7Si composite. No visible pores were observed in all these composites. The inserts in Figs. 2a-d show no evidence of Al_4C_3 formed at the graphite/Al interfaces. The absence of Al_4C_3 is also confirmed by XRD (Fig. 3). Whatever the graphite fillers, only the peaks of graphite, Al and Si are present.

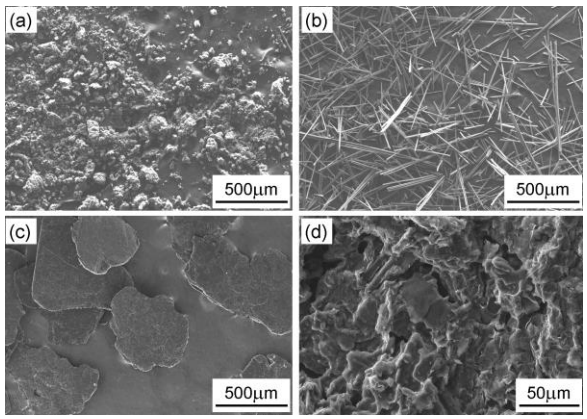

Figure 1. SEM micrographs of the graphite fillers: (a) graphite particles, (b) graphite fibers, (c) graphite flakes and (d) porous graphite block.

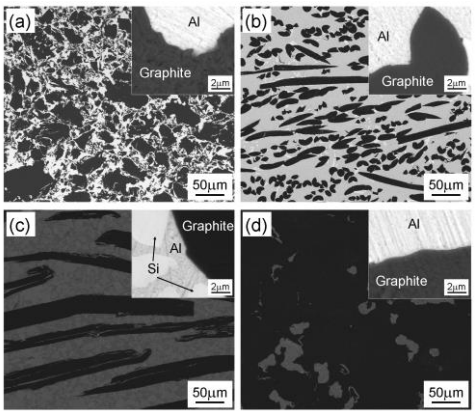

Figure 2. SEM micrographs of the composites obtained from different graphite fillers: (a) graphite particles, (b) graphite fibers, (c) graphite flakes and (d) porous graphite block. Inserts highlight no Al_4C_3 formed at the graphite/Al interfaces.

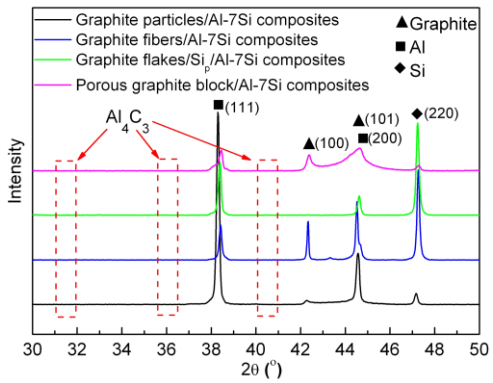

Figure 3. XRD patterns of the graphite/Al-7Si composites. Note that the positions of possible diffraction peaks corresponding to the Al_4C_3 phase are marked in red dotted line boxes.

3.2 Thermal-physical properties of the graphite/Al-7Si composites

The measured thermal-physical properties of the graphite/Al-7Si composites are given in Table 2. The graphite flakes/Si/Al-7Si composites have the highest TC of 504 W/m K. However, it is worth noting that the composites show remarkable anisotropy. Along the *z*-axis of the composites, the TC is only 50 W/m K. Graphite fibers/Al-7Si composites are also anisotropic. The average TC along the *xy*-plane is around 185 W/m K, being almost twice higher than that along the *z*-axis. The anisotropy is attributed to the orientations of flakes and fibers (see Figs. 2b and c). Both the graphite particles/Al-7Si and porous graphite block/Al-7Si composites have isotropic but low TCs. In addition, all of these composites have low densities varying in the range of 2.34-2.45 g/cm^3.

Composites	***f***	**Density [g/cm^3]**	**TC [W/m K]**
Graphite particles/Al-7Si	0.55	2.45	*xyz*: 121
	0.60	2.43	*xyz:* 119
	0.66	2.40	*xyz:* 116
Graphite fibers/ Al-7Si	0.43	2.45	*xy:* 180, *z:* 98
	0.47	2.43	*xy:* 186, *z:* 90
	0.53	2.40	*xy:* 190, *z:* 83
Graphite flakes/Si_p/Al-7Si	0.25	2.40	*xy:* 275, *z:* 80
	0.32	2.39	*xy:* 330, *z:* 70
	0.39	2.38	*xy:* 380, *z:* 62
	0.46	2.36	*xy:* 440, *z:* 56
	0.53	2.35	*xy:* 504, *z:* 50
Porous graphite block/Al-7Si	0.77	2.36	*xyz:* 203
	0.80	2.35	*xyz:* 207
	0.82	2.34	*xyz:* 213

Table 2. Thermal-physical properties of the graphite/Al-7Si composites. The volume fraction (*f*) of the graphite fillers is also reported. *z* refers to the direction along the pressing pressure. The *xy*-plane is denoted by *xy*, which is perpendicular to the *z*-axis. *xyz* indicates the isotropic properties of the materials.

3.3 Predictive schemes for TCs of the graphite/Al-7Si composites

As all the composites present the Al_4C_3-free interface at the micrometric scale (see Fig. 2), the modeling in this study focused on the effect of the observed structure factors of graphite fillers on the TC. There are several models reviewed in Refs. [9-13] for the TC prediction of two- or multi-phase composites. The Maxwell mean-filed (MMF) scheme [13] is a representative approach to solve the TC of randomly distributed and non-interacting homogeneous discrete spheres in homogeneous continuous medium. The experimental data of the graphite particles/Al-7Si composites are quite consistent with the predictions calculated by the MMF scheme (see Fig. 4a). Unidirectional fibers reinforced composites show high one-dimensional TC. However, the experimental TC of the graphite fibers/Al-7Si composites is not as high as expected by the MMF scheme. Here, a theoretical study was carried out within the framework of the effective medium approximation (EMA) [14] and a new model was presented to give reasonable explanation,

considering a two-phase composite containing randomly oriented ellipsoidal fillers embedded in the homogeneous medium. In a previous study reported by Nan *et al.* [14], a general EMA formulation for the TC of arbitrary ellipsoidal particulate composites was derived, which is given as:

$$K_{xy}^{*}=K_m\frac{2+f[\beta_{xy}(1-S_{11})(1+\langle\cos^2\theta\rangle)+\beta_z(1-S_{33})(1-\langle\cos^2\theta\rangle)]}{2-f[\beta_{xy}S_{11}(1+\langle\cos^2\theta\rangle)+\beta_z S_{33}(1-\langle\cos^2\theta\rangle)]},\quad K_z^{*}=K_m\frac{1+f[\beta_{xy}(1-S_{11})(1-\langle\cos^2\theta\rangle)+\beta_z(1-S_{33})\langle\cos^2\theta\rangle]}{1-f[\beta_{xy}S_{11}(1-\langle\cos^2\theta\rangle)+\beta_z S_{33}\langle\cos^2\theta\rangle]} \tag{1}$$

$$\text{with}\quad \beta_{xy}=\frac{K_{11}-K_m}{K_m+S_{11}(K_{11}-K_m)},\quad \beta_z=\frac{K_{33}-K_m}{K_m+S_{33}(K_{33}-K_m)}\quad\text{and}\quad \langle\cos^2\theta\rangle=\frac{\int\rho(\theta)\cos^2\theta\sin\theta d\theta}{\int\rho(\theta)\sin\theta d\theta} \tag{2}$$

where K^* is the TC of the composites, K_m is the TC of the matrix, K is the TC of the inclusion phase, the subscripts *xy* and *z* denote the directions of thermal conduction, f is the volume fraction of the inclusion phase, θ is the angle between the materials axis (i.e. the *z*-axis) and the local symmetric axis of the inclusion, $\rho(\theta)$ is a distribution function describing ellipsoidal inclusion orientation, and S_{ii} are well-known geometrical factors of the inclusion dependent on the aspect ratio p and given by [15]:

$$S_{11}=S_{22}=\begin{cases}\dfrac{p^2}{2(p^2-1)}-\dfrac{p^2}{2(p^2-1)^{3/2}}\cosh^{-1}p, & p>1\\[2ex] \dfrac{p^2}{2(p^2-1)}+\dfrac{p^2}{2(1-p^2)^{3/2}}\cos^{-1}p, & p<1\end{cases}\quad\text{and}\quad S_{33}=1-2S_{11} \tag{3}$$

Changes can be brought to the EMA formulation to account for TC of the graphite fibers/Al-7Si composites. It is noted that these cylindrical fibers used in this work have a very high aspect ratio (~40), thus approximately, S_{11}=S_{22}=0.5 and S_{33}=0 [16]. Considering that most of the graphite fibers are highly oriented in the *xy*-plane of the composites and the composite has ∞mm symmetry, then $<\cos^2\theta>\rightarrow 0$, and thus the expressions (Eq. (1)) reduce to:

$$K_{xy}^{*}=K_m\frac{4+f(\beta_{xy}+2\beta_z)}{4-f\beta_{xy}}\quad\text{and}\quad K_z^{*}=K_m\frac{2+f\beta_{xy}}{2-f\beta_{xy}} \tag{4}$$

However, $<\cos^2\theta>$ is slightly greater than zero due to the imperfect orientation as shown in Fig. 2b. It should be noted that the accurate value of $<\cos^2\theta>$ is technically difficult to measure. A simple and effective model is imperative and needs to be developed. To this end, an experiential factor A is introduced to the Eq. (4), and thus the expressions reduce to:

$$K_{xy}^{*}=A_{xy}K_m\frac{4+f(\beta_{xy}+2\beta_z)}{4-f\beta_{xy}}\quad\text{and}\quad K_z^{*}=A_zK_m\frac{2+f\beta_{xy}}{2-f\beta_{xy}} \tag{5}$$

The factor A mainly depends on the pressing pressure applied to prepare the preform. In our case, A_{xy}=0.9 and A_z=1.4, which are achieved from experiments. Comparison between the experimental data of the graphite fibers/Al-7Si composites and the predictions by the present model is shown in

Fig. 4b. Apparently, the predictions by using Eq. (5) are in excellent agreement with the experimental data in the directions along the *xy*-plane and the *z*-axis. For the composites with embedded graphite flakes highly oriented in the *xy*-plane, thus $< \cos^2\theta > \rightarrow 1$, then the EMA formulations reduce to:

$$K_{xy}^{*} = K_m + \frac{fK_m}{S_{11}(1-f) + \frac{K_m}{K_{xy} - K_m}} \quad \text{and} \quad K_z^{*} = K_m + \frac{fK_m}{S_{33}(1-f) + \frac{K_m}{K_z - K_m}} \tag{6}$$

Approximately regarding the shape of graphite flakes as a disc, the geometrical factors can be then expressed as, $S_{11}=S_{22}=\pi p/4$ and $S_{33}=1-\pi p/2$ [16]. The TC of the matrix (Si/Al-7Si materials) was 104 W/m K measured by experiment. Comparison between the experimental data of the graphite flakes/Si_p/Al-7Si composites and the EMA predictions is also shown in Fig. 4. The EMA predictions are in good agreement with the experimental data. The K^{*}_{xy} of the graphite flakes/Si_p/Al-7Si composites are higher than that of the graphite fibers/Al-7Si composites, while the K^{*}_{z} is relatively low. In the case of the porous graphite block/Al-7Si composite, porous graphite block has interconnected open pores and can be initially regarded as a binary composite with graphite matrix and air. After being infiltrated with Al-7Si alloy, these pores are replaced by the metal network structure. Consequently, the thermal properties of this composite are enhanced due to relatively high TC of Al alloy compared to the air in the pores. As the graphite block has a TC close to the Al alloy, we regarded the interpenetrating porous graphite block/Al-7Si composite as a particle-reinforced composite and use the MMF scheme for theoretical calculations. First, taking the apparent TC (see Table 1) as the TC of the binary composite, we derived the intrinsic TC value of the graphite matrix of 223 W/m K using the Maxwell equation. Then, we introduced this value into the Maxwell equation again, and obtained the TC of the porous graphite block/Al-7Si composite, namely, 209 W/m K. The value is very close to the experimental data of 213 W/m K. The comparison of the experimental data and the predictions by the MMF scheme is shown in Fig. 4a. The theoretical predictions are in agreement with the experimental data, which confirms the validity of this scheme.

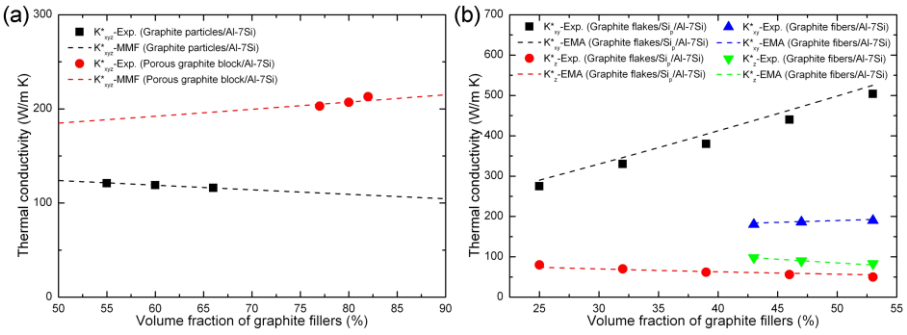

Figure 4. Comparison between the experimental TC data and the predictions for: (a) the graphite particles/Al-7Si and porous graphite block/Al-7Si composites; (b) the graphite flakes/Si/Al-7Si and graphite fibers/Al-7Si composites.

3.4 The potentials of these graphite fillers in thermal enhancement

In order to evaluate the potentials of these graphite fillers in thermal enhancement, a numerical computation for the TC of the composites (K^*_{xyz} or K^*_{xy}) with different graphite fillers content was performed. The comparisons of the potentials of these composites are shown in Fig. 5. For the graphite particles/Al-7Si composite (Fig. 5a), highly conductive graphite particles are the key to achieve the high TC of the composites. However, the commercially available graphite particles have very low TC since defects and impurities may considerably reduce their thermal properties [2]. Thus, it is infeasible to achieve high thermal properties using graphite particles. As shown in Fig. 5b, the graphite fibers have a low potential. Even if the fibers with a superior high TC (900-1100 W/m K) are used, the TC of the composites is still unsatisfactory (~300 W/m K). Compared with graphite fibers, graphite flakes show higher in-plane TC enhancement. The in-plane TC of the graphite flakes/Si/Al-7Si composites can compete favorably with commercially available diamond/Cu composites (TC = 470 W/m K) [2]. Finally, the porous graphite block also shows a good potential. As shown in Fig. 5a, the TC of the porous graphite block/Al-7Si composites is relatively higher than the graphite block itself. It is known that the intrinsic TC of the graphite block increases with the increase of porosity (i.e. inversely proportional to the volume fraction of graphite matrix). This is the reason why the TC of the composites decreases with the increasing graphite volume fraction. In summary, the graphite flakes/Si/Al-7Si and porous graphite block/Al-7Si composites show enhanced TCs, which make them promising materials for thermal management applications.

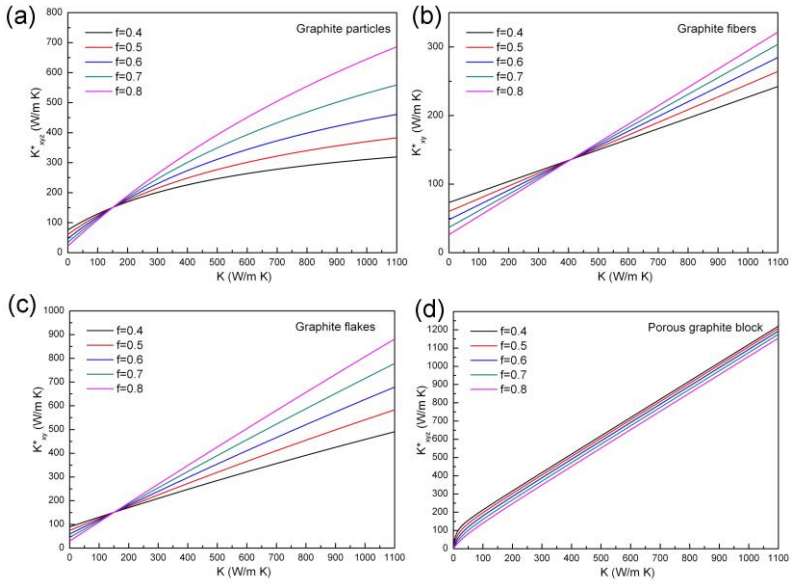

Figure 5. Numerical computation for the effect of the TC of graphite fillers (K) on the overall TC of the composites (K^*_{xyz} or K^*_{xy}): (a) graphite particles, (b) graphite fibers, (c) graphite flakes and (d) porous graphite block.

4. Conclusions

Various graphite/Al-7Si composites have been fabricated by squeeze casting. Microstructure characterization confirmed a clean and Al_4C_3-free interface between the graphite and the aluminum matrix. The EMA approach has a high predictive capacity for the graphite fibers/Al-7Si

and graphite flakes/Si/Al-7Si composites, while the MMF scheme can be suitable to predict the TCs of the graphite partcles/Al-7Si and porous graphite block/Al-7Si composites. The numerical computation of the TCs of these composites also indicates that the oriented graphite flakes alignment and porous graphite block have the optimal structure factors for high TC enhancement, which make them promising reinforcement materials for thermal management applications.

References

[1] S. Mallik, N. Ekere, C. Best, R. Bhatti. Investigation of thermal management materials for automotive electronic control units. Applied Thermal Engineering, 31(2-3):355-362, 2011.

[2] R. Prieto, J. M. Molina, J. Narciso, E. Louis. Fabrication and properties of graphite flakes/metal composites for thermal management applications. Scripta Materialia, 59(1):11-14, 2008.

[3] T. Ueno, T. Yoshioka, J. I. Ogawa, N. Ozoe, K. Sato, K. Yoshino. Highly thermal conductive metal/carbon composites by pulsed electric current sintering. Synthetic Metals, 159(21-22):2170-2172, 2009.

[4] R. Prieto, J. M. Molina, J. Narciso, E. Louis. Thermal conductivity of graphite flakes-SiC particles/metal composites. Composites: Part A, 42(12):1970-1977, 2011.

[5] J. K. Chen and I. S. Huang. Thermal properties of aluminum–graphite composites by powder metallurgy. Composites: Part B, 44(1):698-703, 2013.

[6] T. Etter, P. Schulz, M. Weber, J. Metz, M. Wimmler, J. F. Löffler, P. J. Uggowitzer. Aluminum carbide formation in interpenetrating graphite/aluminium composites. Materials Science and Engineering A, 448(1-2):1-6, 2007.

[7] L. Hu, T. Desai, P. Keblinski. Thermal transport in graphene-based nanocomposite. Journal of Applied Physics, 110(3):033517, 2011.

[8] C. Zhou, G. Ji, Z. Chen, M. L. Wang, A. Addad, D. Schryversc, H. W. Wang. Fabrication, interface characterization and modeling of oriented graphite flakes/Si/Al composites for thermal management applications. under review.

[9] L. P. Kollar and G. S. Springer. Mechanics of Composite Structure, Cambridge University Press, Cambridge, 2003.

[10] J. C. Maxwell. A Treatise on Electricity and Magnetism, Clarendon Press, Oxford, 1891.

[11] L. Rayleigh. On the influence of obstacles arranged in rectangular order upon the properties of a medium. Philosophical Magazine, 34(211):481-501, 1892.

[12] T. W. Clyne. Thermal and Electrical Conduction in MMCs. In C. Zweben, A. Kelly, editors, Comprehensive Composite Materials, 447-468. Elsevier, Oxford, 2000.

[13] D.P.H. Hasselman and L.F. Johnson. Effective thermal conductivity of composites with interfacial thermal barrier resistance. Journal of Composite Materials, 21(6):508-515, 1987.

[14] C. W. Nan, R. Birringer, D. R. Clarke, H. Gleiter. Effective thermal conductivity of particulate composites with interfacial thermal resistance. Journal of Applied Physics, 81(10):6692-6699, 1997.

[15] C. W. Nan. Effective-medium theory of piezoelectric composites. Journal of Applied Physics, 76(2):1155-1163, 1994.

[16] H. Hatta and M. Taya. Equivalent inclusion method for steady state heat conduction in composites. International Journal of Engineering Science, 24(7):1159-1172, 1986.